Performance Analysis of FS-FBMC/OQAM System Using Turbo and LDPC Codes

Anam Mobin and Anwar Ahmad
Department of Electronics and Communication Engineering, Jamia Millia Islamia, New Delhi, 110025, India
Email: anammobin92@gmail.com, aahmad4@jmi.ac.in

Abstract—Filter Bank Multicarrier (FBMC) with offset QAM (OQAM) is a possible waveform candidate for 5G and future wireless systems and standards. FBMC is realized using either polyphase network (PPN)-FFT or Frequency Spread (FS)-FBMC. In this paper, channel coding schemes such as turbo codes and low-density parity check (LDPC) codes were investigated in terms of their peak-to-average power ratio (PAPR) and bit-error-rate (BER) reduction performances for FS-FBMC/OQAM and Orthogonal Frequency Division Multiplexing (OFDM) systems in additive white Gaussian noise (AWGN) channel. Simulation results show that turbo coded and LDPC coded FS-FBMC/OQAM systems performed better than turbo coded and LDPC coded OFDM systems in terms of BER performance. Also, LDPC coded FS-FBMC/OQAM system because of its adequate BER performance, reasonable PAPR performance, and reduced computational complexity was found to be an appropriate choice among other systems for 5G and future wireless networks. It was also found that incorporating channel coding resulted in a very large coding gain with only a minor rise in the system's PAPR value.

Index Terms—Filter Bank Multicarrier (FBMC), Orthogonal Frequency Division Multiplexing (OFDM), offset QAM (OQAM), turbo codes, low-density parity check (LDPC) codes

I. Introduction

Filter Bank Multicarrier (FBMC) is a possible multicarrier waveform candidate for 5G and future wireless systems and standards. It offers several advantages such as minimum out-of-band (OOB) leakage among other multicarrier waveform candidates such as Filtered-OFDM (F-OFDM), Generalized Frequency Division Multiplexing (GFDM), and Universal Filtered Multi-carrier (UFMC), high spectral efficiency, and relaxed synchronization requirements [1], [2].

Channel coding enhances the reliability of a system but at the cost of increased system complexity and extra bandwidth requirement. In [3] performance of turbo coded Orthogonal Frequency Division Multiplexing (OFDM) and FBMC systems are investigated in the presence of phase noise. In [4], a turbo coded MIMO-FBMC system is proposed and compared with a turbo coded MIMO-OFDM system. In [5], BER performance of turbo coded and uncoded massive MIMO-FBMC system is compared with turbo coded and uncoded massive MIMO-OFDM system in underwater acoustic channel for real-time video transmission. In [6], authors have proposed a parallel coding technique using turbo product code for mobile multimedia data transmission over a MIMO-FBMC system. In [7], performance of low-density parity check (LDPC) coded FBMC system is investigated. In [8], authors have proposed a LDPC coded FBMC system for data transmission over underwater acoustic channel. In [9], non-binary LDPC codes are applied to FBMC/OQAM system. In [10], authors have proposed a LDPC coded MIMO-FBMC system for multimedia signals transmission over underwater acoustic channel. In [11], authors have proposed a LDPC coded FBMC system for voice and image transmission over underwater acoustic channel.

FBMC can be realized either using polyphase network (PPN)-FFT or Frequency Spread (FS)-FBMC realization [12]. In this work FS-FBMC realization is employed.

In this paper turbo coded and LDPC coded FS-FBMC/OQAM systems were investigated and compared in terms of peak-to-average power ratio (PAPR) performance and bit-error-rate (BER) performance over additive white Gaussian noise (AWGN) channel, which was not studied in any of the earlier works. Also, turbo coded and LDPC coded OFDM systems were compared with turbo coded and LDPC coded FS-FBMC/OQAM systems in terms of PAPR and BER performances. It was observed that turbo coded and LDPC coded FS-FBMC/OQAM systems outperformed turbo coded and LDPC coded OFDM systems, with turbo coded FS-FBMC/OQAM systems outperforming other systems in the signal-to-noise ratio (SNR) range of -4 dB to -2 dB and LDPC coded FS-FBMC/OQAM systems outperforming other systems for -2 dB < SNR ≤ -1 dB. For SNR > -1dB, turbo coded FS-FBMC/OQAM system, LDPC coded FS-FBMC/OQAM system, and turbo coded OFDM system all provided BER=0. Also, it was found that LDPC coded FS-FBMC/OQAM system provided reasonable PAPR performance and reduced computational complexity.

This work is organized as follows: Section II defines an OFDM system. Section III introduces the FS-FBMC/OQAM system. PAPR of FS-FBMC/OQAM signal is defined in Section IV. Turbo codes and LDPC codes are presented in Section V. The proposed coded FS-FBMC/OQAM system is shown in Section VI. Section VII contains the simulation results as well as a discussion of the findings. Conclusions are drawn in Section VIII based on the findings.

Manuscript received January 10, 2022; revised July 12, 2022.
Corresponding author email: anammobin92@gmail.com
doi:10.12720/jcm.17.8.661-667

II. OFDM System

OFDM is a multi-carrier modulation system in which data is sent as a combination of orthogonal narrowband signals known as subcarriers. OFDM is based on single carrier modulation, like QAM, and can transmit data at similar rates. OFDM, on the other hand, is more resistant to frequency selective fading and allows for easier receiver equalization. Many common wireless communication technologies, including WiFi and LTE, use OFDM as a basic architecture.

The OFDM transmission method is made up of numerous different parts. The information is first coded and modulated, most commonly into QAM symbols. These symbols are fed into equally spaced frequency bins, and the signal is transformed into orthogonal overlapping sinusoids in the time domain using the inverse fast Fourier transform (IFFT).

One OFDM symbol is made up of the N samples at the IFFT's output. Each OFDM symbol is then given a cyclic prefix (CP), which permits circular convolution to be computed using linear convolution if the CP is at least as long as the channel impulse response. This enables receiver equalization to reduce intersymbol interference using a simple complex scalar multiplication applied to each OFDM symbol separately.

OFDM due to its certain disadvantages such as low spectral efficiency due to redundant CP transmission, high OOB leakage due to rectangular pulse shaping, and requirement of strict frequency synchronization between subcarriers is not a suitable choice for 5G systems [13].

III. FS-FBMC/OQAM System

FBMC is a multicarrier waveform method in which non-rectangular pulse shaping filters are used to filter the individual subcarriers. Over K symbol intervals, the FBMC symbol expands. As a result, it overlaps with K successive FBMC symbols. The overlapping factor is denoted by the letter K. Fig. 1 [13] illustrates the FS-FBMC/OQAM transceiver structure. Time domain subcarrier multi tap equalization is required by the PPN-FFT FBMC receiver, which adds to the transmission latency. For each subcarrier, the FS-FBMC receiver requires only one tap frequency domain equalization, which results in no additional delay. The FS-FBMC transceiver requires KN-sized extended IFFT and FFT.

The total number of subcarriers is N in this case. The PPN-FFT transceiver requires N-size IFFT and FFT, as well as KN additional multiplications for the PPN [14].

The following equation can be used to explain the frequency spreading [12] operation:

$$S_{lK+k} = F_k \times d_l \tag{1}$$

where, $S(p')$ has index $lK + k$ and $d(p)$ has index l, and $d(p)$ is a sequence of real and imaginary parts (imaginary parts are multiplied by imaginary term 'j') of complex modulated symbols that alternate to ensure real field orthogonality across subcarriers $S(p')$, and F_k are the frequency domain coefficients of prototype filter such that $F_k = F_{-k}$.

Here, p=0 to N-1, l=1 to N, p′= 0 to KN-1, and k= -(K-1) to (K-1).

The following equation can be used to express the output of the extended IFFT block, s(n'):

$$s(n') = \frac{1}{\sqrt{KN}} \sum_{p'=0}^{KN-1} S(p') e^{\,j2\pi p' n'/KN} \tag{2}$$

where, n′=0 to KN-1

To achieve full capacity, OQAM is used to double the symbol rate. By switching the mapping of the real and imaginary parts of complex modulated symbols at the frequency spreading and filtering block's inputs, successive extended IFFT outputs can be formed. Extended IFFT outputs having a duration of KN are overlapped with a delay of N/2, then summed and sent across a channel. The time domain output of the FS-FBMC/OQAM transmitter is shown in Fig. 2 and can be expressed as follows:

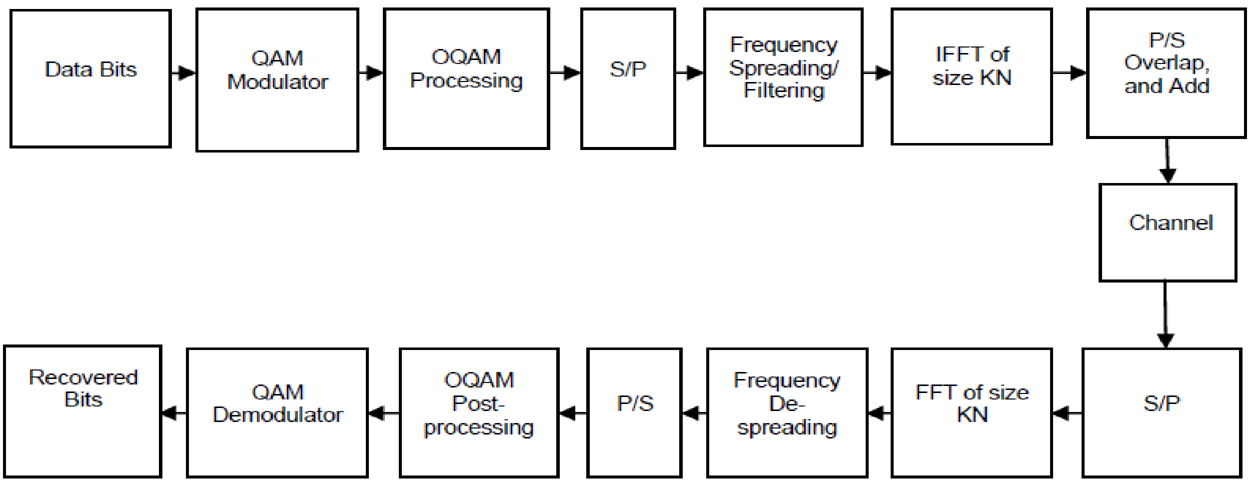

Fig. 1. FS-FBMC/OQAM transceiver block diagram.

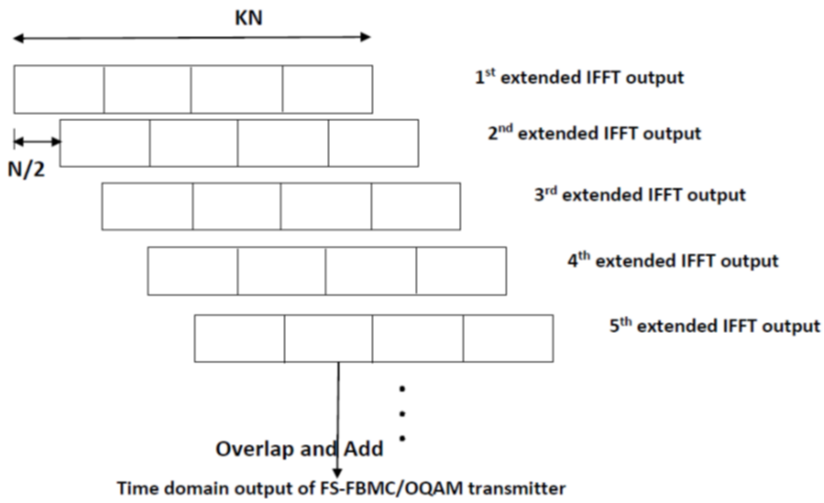

Fig. 2. Output of FS-FBMC/OQAM transmitter.

$$x_{FBMC}(n) = \sum_{(g=0)}^{(T_0-1)} s_g(n - gN/2) \tag{3}$$

where, $n = 0\ to\ (K + T_0/2)\ N - N/2 - 1$

Where, T_0 is the total number of FS-FBMC/OQAM symbols, and $s_g(n')$ is the g^th extended IFFT output.

The received FS-FBMC/OQAM signal $r_{FBMC}(n)$ is expressed as:

$$r_{FBMC}(n) = x_{FBMC}(n) + w(n) \tag{4}$$

where, the channel noise signal is denoted by w(n).

The first FS-FBMC/OQAM symbol is $r_{FBMC}(n)|_{n=0\ to\ KN-1}$, the second FS-FBMC/OQAM symbol is $r_{FBMC}(n)|_{n=KN\ to\ 2KN-1}$, and so on.

The following equation can be used to explain the frequency de-spreading [12] operation conducted at the receiver side:

$$d_l^{'} = \sum_{k=-(K-1)}^{K-1} S'_{lK+k} \times F_k \tag{5}$$

where, the frequency de-spreading and filtering block's outputs are $d^{'}(p)$ indexed as l, while the frequency de-spreading and filtering block's inputs are $S'(p')$ with index $lK + k$.

IV. Peak-to-Average Power Ratio (PAPR)

PAPR of FS-FBMC/OQAM signal x[n] can be expressed as:

$$PAPR(dB) = 10\ log_{10}\left(\frac{max_{\ 0\le n\le KN-1}\ |x[n]|^2}{E[|x[n]|^2]}\right) \tag{6}$$

where, $x(n) = x_{FBMC}(n)|_{n=0\ to\ KN-1}$

The complementary cumulative distribution function (CCDF) of PAPR values is defined as the probability, P, that PAPR exceeds some predetermined limit, $PAPR_0$, and is stated as:

$$CCDF(PAPR_0) = P(PAPR > PAPR_0) \tag{7}$$

V. Channel Codes

A. Turbo Codes

A turbo encoder is a recursive systematic encoder with two concurrent recursive systematic convolutional encoders [15]. After applying a pseudorandom interleaving technique to the input bit sequence, it is transmitted through the second convolutional encoder.

For a particular number of iterations, turbo decoding employs one of the two algorithms: Log-Maximum A Posteriori (MAP) or Max-Log-MAP [15].

An iterative Max-Log-MAP turbo decoding technique, a simplified version of Log-MAP, is used here.

Turbo codes with large interleavers have some drawbacks, such as increased decoding delay and a computationally complex iterative decoding procedure. However, most communication systems tolerate the decoding delay and increased computational complexity in order to achieve very high coding gain [15].

WCDMA, LTE, DVB, and WiMAX all use turbo codes [16], [17].

B. LDPC Codes

The Low-Density Parity Check (LDPC) code is a linear error-correction code with a sparse parity check matrix H (fewer nonzero elements in each column and row of the matrix, H) [18]. There are two approaches to represent LDPC codes: one using a parity check matrix, H, and the other using a graphical representation, such as a bipartite graph [19].

If the length of a code word is represented by n_0, the number of information bits is represented by k_0, and the number of parity bits is represented by m_0, then the code rate is $R_c = k_0/\ n_0$. If u stands for uncoded input bits, the codeword c is written as [19]:

$$c = uG \tag{8}$$

where,

$$G_{k_0 \times n_0} = [I_{k_0} P_{k_0 \times (n_0 - k_0)}] \quad (9)$$

G is the generator matrix of size $k_0 \times n_0$, I_{k_0} is the identity matrix of size $k_0 \times k_0$ and P is parity matrix of size $k_0 \times (n_0 - k_0)$. H stands for Parity Check Matrix and is expressed as [19]:

$$H_{(n_0 - k_0) \times n_0} = [P^T \; I_{n_0 - k_0}] \quad (10)$$

Because the matrices G and H are orthogonal [19]:

$$HG^T = 0 \quad (11)$$

The LDPC decoder employs either soft or hard decision decoding algorithms. Soft decision decoding techniques have a significant improvement in BER performance, but at the expense of higher computational complexity and decoding delay. Hard decision decoding methods have a shorter decoding delay but a lower BER performance [19].

The soft decision hard output iterative Belief Propagation decoding algorithm [19] is utilized in this study since it has a low computational complexity and decoding time.

DVB-S2, WiMAX 802.16e, Wireless LAN 802.11n, and Wireless RAN 802.22 [18], [19] all employ LDPC codes. LDPC codes are also candidates for 5G channel codes [19].

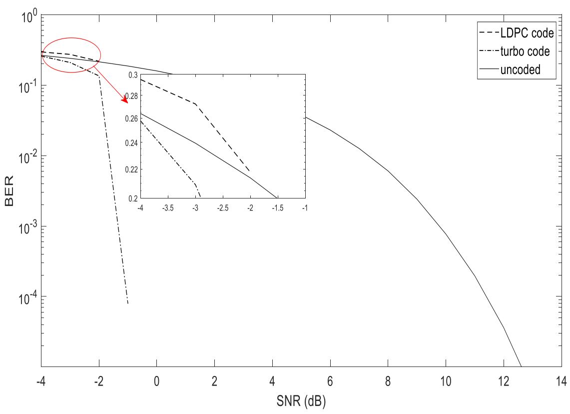

Fig. 3. BER performance of turbo and LDPC codes using 4-QAM in AWGN channel for code rate, Rc=1/3.

Fig. 3 depicts the BER performance of turbo and LDPC codes in AWGN channel using 4-QAM for code rate, R_c=1/3. It can be observed that turbo code provides better BER performance in the SNR range of -4 dB to -2 B. Also, it can be observed that turbo code provides BER=0 for SNR > -1 dB, whereas LDPC code provides BER=0 for SNR > -2 dB.

TABLE I: PARAMETER VALUES OF LDPC CODES AND TURBO CODES

	Parameters	Values
LDPC code	Code rate, R_c	1/3
	Parity check matrix, H	As used in DVB-S2 standard
Turbo code	Code rate, R_c	1/3
	Constraint length	4
	Generator matrix	$[13\ 15]_{octal}$

VI. PROPOSED CODED FS-FBMC/OQAM SYSTEM

The proposed coded FS-FBMC/OQAM system is depicted in Fig. 4 as a block diagram employing either turbo codes or LDPC codes. The random data bits are encoded using a turbo encoder or an LDPC encoder, then modulated using an FS-FBMC/OQAM modulator, as described in Section III. The FS-FBMC/OQAM signal is then passed through the AWGN channel. The received FS-FBMC/OQAM symbols are first demodulated at the receiver using the FS-FBMC/OQAM demodulator (described in Section III), and then the data bits are decoded using either the turbo decoder or the LDPC decoder (covered in Section III). On the receiver side, perfect channel estimation is assumed.

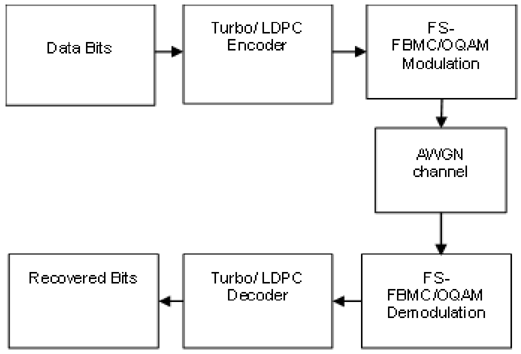

Fig. 4. Proposed coded FS-FBMC/OQAM system.

The total number of operations (Additions, Multiplications, Complex operations) per code word for turbo, and LDPC codes, can be expressed using (12) and (13) respectively [20]:

$$T_{turbo} \cong 5 \times 10^4 L \quad (12)$$

where, T_{turbo} is the total number of operations per code word for turbo codes, and L is the codeword length.

$$T_{LDPC} \cong 0.8 \times 10^4 L \quad (13)$$

where, T_{LDPC} is the total number of operations per code word for LDPC codes. Hence, in comparison to turbo decoding, LDPC decoding takes less operations per code word length:

$$T_{turbo} \cong 6\, T_{LDPC} \quad (14)$$

VII. SIMULATION RESULTS

In the AWGN channel, the suggested coded FS-FBMC/OQAM system was evaluated in terms of PAPR and BER performances. N′=22024 was chosen as the number of uncoded subcarriers, while N=65224 was chosen as the number of coded subcarriers. The number of subcarriers allocated to guard band was set at 424. K=4 was chosen as the overlapping factor. The prototype filter's frequency domain coefficients, F_k, were utilized as specified in the PHYDYAS project [12]. The modulation scheme used was 4-QAM. Table I shows the parameter values of LDPC, and turbo codes used in this work. Soft decision hard output Max-Log-MAP decoding algorithm was used for turbo decoding with 4 iterations. Soft decision hard output Belief Propagation decoding algorithm was used for LDPC decoding with maximum number of iterations set to 50. MATLAB was used to carry out the simulations.

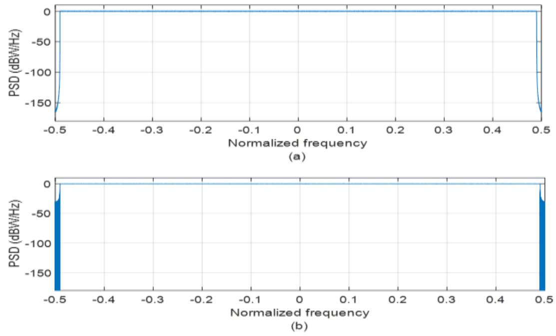

Fig. 5. (a) PSD of uncoded FS-FBMC/OQAM signal (b) PSD of uncoded OFDM signal

TABLE II: PAPR PERFORMANCE COMPARISON OF UNCODED FS-FBMC/OQAM AND OFDM SYSTEMS

	OFDM	FS-FBMC/OQAM
PAPR (dB) at CCDF=10^{-4}	11.38	11.84

Fig. 5 (a) and Fig. 5 (b) show the power spectral density (PSD) plots of uncoded FS-FBMC/OQAM and OFDM systems, respectively. Here, the no. of subcarriers was fixed at 22024 for both uncoded FS-FBMC/OQAM and uncoded OFDM systems and the number of overlapped symbols, K was fixed at 4 for uncoded FS-FBMC/OQAM system. Table II compares the PAPR performance of uncoded FS-FBMC/OQAM and OFDM systems. Fig. 6 shows the BER performance of uncoded FS-FBMC/OQAM and OFDM systems in the AWGN channel for various SNR values. It can be observed that uncoded OFDM and FS-FBMC/OQAM systems provide almost similar PAPR and BER performances, but FS-FBMC/OQAM system provides very low OOB emission as compared to OFDM system ($PSD_{FS\text{-}FBMC/OQAM} \approx -175$ dBW/Hz, and $PSD_{OFDM} \approx -30$ dBW/Hz at Normalized Frequency=0.5). Also, FS-FBMC/OQAM system provides high spectral efficiency as compared to OFDM system because of no CP transmission.

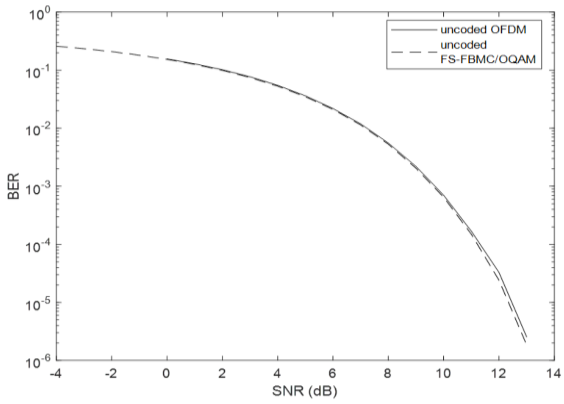

Fig. 6. BER performance of uncoded FS-FBMC/OQAM and uncoded OFDM systems in AWGN channel.

Fig. 7 shows the BER performance of turbo and LDPC coding schemes for FS-FBMC/OQAM systems in the AWGN channel for various SNR values. It can be shown that turbo coded FS-FBMC/OQAM system provided somewhat better BER performance than LDPC coded FS-FBMC/OQAM system in the SNR range of -4 dB to -2 dB. The LDPC coded FS-FBMC/OQAM system, however, outperformed the turbo coded FS-FBMC/OQAM system for -2 dB < SNR ≤ -1 dB, providing BER=0 for SNR > -2 dB. In contrast, the turbo coded FS-FBMC/OQAM system provides BER=0 for SNR > -1 dB. For SNR > -1dB, both turbo coded and LDPC coded FS-FBMC/OQAM systems provided BER=0.

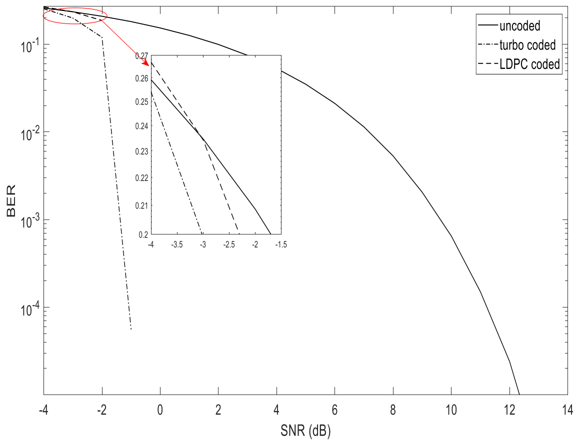

Fig. 7. BER performance of turbo and LDPC coding schemes for FS-FBMC/OQAM system in AWGN channel.

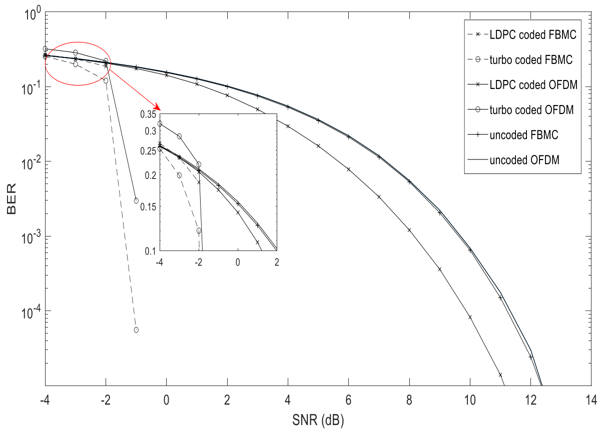

Fig. 8. BER performance of turbo and LDPC coding schemes for OFDM and FS-FBMC/OQAM systems in AWGN channel.

Fig. 8 shows the BER performance of turbo and LDPC coding schemes for OFDM and FS-FBMC/OQAM systems in the AWGN channel for various SNR values. Turbo coded and LDPC coded FS-FBMC/OQAM systems outperformed turbo coded and LDPC coded OFDM systems, with turbo coded FS-FBMC/OQAM systems outperforming other systems in the SNR range of -4 dB to -2 dB and LDPC coded FS-FBMC/OQAM systems outperforming other systems for -2 dB < SNR≤ -1 dB. For SNR > -1dB, turbo coded FS-FBMC/OQAM system, LDPC coded FS-FBMC/OQAM system, and turbo coded OFDM system all provided BER=0. Table 3 shows the

PAPR performance of different coded systems. It can be observed that LDPC coded OFDM system outperforms other systems in terms of PAPR performance, but it is not an appropriate choice because it provides inadequate BER performance as compared to other coded systems as shown in Fig. 8. It can be observed that LDPC coded FS-FBMC/OQAM system provides a lower PAPR value in addition to acceptable BER performance. From Table II and Table III, it can also be observed that the inclusion of channel coding increases the PAPR value of the system (by about 2 dB) but at the same time provides a very high coding gain of about 14 dB at BER=0 as shown in Fig. 7.

TABLE III: PAPR VALUES OBTAINED USING DIFFERENT CODED SYSTEMS

Proposed Systems	PAPR (dB) at CCDF=10^{-4}
Turbo coded FS-FBMC/OQAM	13.46
LDPC coded FS-FBMC/OQAM	12.83
Turbo coded OFDM	13.42
LDPC coded OFDM	12.69

Also, it can be stated that LDPC coded FS-FBMC/OQAM can be used for applications that require less computational complexity and decoding latency, because in comparison to turbo decoding, LDPC decoding takes less operations per code word length as shown in (14).

VIII. CONCLUSION

In this paper, uncoded and coded FS-FBMC/OQAM and OFDM systems were analyzed in AWGN channel in terms of BER and PAPR performances. It was observed that uncoded FS-FBMC/OQAM and OFDM systems provided similar BER and PAPR performances, but FS-FBMC/OQAM system provided very low OOB leakage and high spectral efficiency as compared to OFDM system. Also, turbo coded and LDPC coded FS-FBMC/OQAM systems outperformed turbo coded and LDPC coded OFDM systems in terms of BER performance. It was also observed that LDPC coded FS-FBMC/OQAM system provided reasonable PAPR performance along with acceptable BER performance, reduced computational complexity and decoding latency. Hence, LDPC coded FS-FBMC/OQAM system due to its advantages is found to be an appropriate multicarrier waveform technique for 5G and future wireless networks. Also, incorporation of channel coding provided a very high coding gain with a small increase in the PAPR value of the system.

CONFLICT OF INTEREST

The authors declare no conflict of interest.

AUTHOR CONTRIBUTIONS

Conceptualization: Anam Mobin, Anwar Ahmad; Methodology: Anam Mobin; Formal analysis and investigation: Anam Mobin; Writing—original draft preparation: Anam Mobin; Writing—review and editing: Anam Mobin; Resources: Anwar Ahmad; Supervision: Anwar Ahmad.

REFERENCES

[1] N. Maziar, W. Yue, T. Milos, W. Shangbin, Q. Yinan and A. Mohammed, “Overview of 5G modulation and waveforms candidates,” *Journal of Communications and Information Networks*, vol. 1, no. 1, pp. 44-60, June 2016.

[2] Y. Cai, Z. Qin, F. Cui, G. Y. Li, and J. A. McCann, “Modulation and multiple access for 5G networks,” *IEEE Communications Surveys & Tutorials*, vol. 20, no. 1, pp. 629-646, 2018.

[3] K. Roth, L. G. Baltar, M. Faerber, and J. A. Nossek, “Performance analysis of FBMC and CP-OFDM in the presence of phase noise,” in *Proc. European Conference on Networks and Communications (EuCNC)*, 2017, pp. 1-5.

[4] L. Mathews and S. S. Pillai, “Performance of turbo coded FBMC based MIMO systems,” in *Proc. IEEE International Conference on Computational Intelligence and Computing Research (ICCIC)*, 2016, pp. 1-5.

[5] M. J. Bocus, D. Agrafiotis, and A. Doufexi, “Real-time video transmission using massive MIMO in an underwater acoustic channel,” in *Proc. IEEE Wireless Communications and Networking Conference (WCNC)*, 2018, pp. 1-6.

[6] Z. Li, M. Miao, and Z. Wang, “Parallel coding scheme with turbo product code for mobile multimedia transmission in MIMO-FBMC system,” *IEEE Access*, vol. 8, pp. 3772-3780, 2020.

[7] S. Jo and J. S. Seo, “Tx scenario analysis of FBMC based LDM system,” *ICT Express*, vol. 1, no. 3, pp. 138-142, 2015.

[8] C. F. Lin, T. J. Su, S. H. Chang, I. A. Parinov, and S. N. Shevtsov, “Direct mapping based FBMC-LDPC advanced underwater acoustic transmission scheme for data signals,” in *Advanced Materials*, Springer, Cham, 2020, pp. 597-603.

[9] M. Caus, M. Navarro, X. Mestre, and A. Pérez-Neira, “Link adaptation in FBMC/OQAM systems using NB-LDPC codes,” in *Proc. European Conference on Networks and Communications (EuCNC)*, 2016, pp. 11-15.

[10] C. F. Lin, T. J. Su, H. K. Chang, C. K. Lee, S. H. Chang, I. A. Parinov, and S. Shevtsov. “Direct-mapping-based MIMO-FBMC underwater acoustic communication architecture for multimedia signals,” *Applied Sciences*, vol. 10, no. 1 pp. 233, 2020.

[11] C. F. Lin, Y. T. Hung, H. W. Lu, S. H. Chang, I. A. Parinov, and S. Shevtsov, “FBMC/LDPC-based underwater transceiver architecture for voice and image transmission,” *Journal of Marine Science and Technology*, vol. 26, no. 3, pp. 4, 2018.

[12] M. Bellanger, D. L. Ruyet, D. Roviras, M. Terré, J. Nossek, L. Baltar, Q. Bai, D. Waldhauser, M. Renfors, and T. Ihalainen. “FBMC physical layer: A primer,” *PHYDYAS*, vol. 25, no. 4 pp. 7-10, January 2010.

[13] A. Mobin and A. Ahmad, “PAPR reduction of FBMC-OQAM systems using logarithmic rooting companding,” in *Proc. Fourth International Conference on Electrical, Computer and Communication Technologies (ICECCT)*, 2021, pp. 1-6.

[14] M. Bellanger, “FS-FBMC: A flexible robust scheme for efficient multicarrier broadband wireless access,” in *Proc. IEEE Globecom Workshops*, 2012, pp. 192-196.

[15] J. G. Proakis, and M. Salehi, *Digital Communications*, vol. 4, New York: McGraw-hill, 2001.

[16] C. Berrou, R. Pyndiah, P. Adde, C. Douillard, and R. L. Bidan, “An overview of turbo codes and their applications,”

in *Proc. European Conference on Wireless Technology, 2005.*, 2005, pp. 1-9.
[17] X. Long, Q. Chen, P. Xiao, and J. Wu, "On the design of PS-RCPT codes for LTE system," in *Proc. IEEE Global Communications Conference (GLOBECOM)*, 2012, pp. 4238-4243.
[18] Z. R. M. Hajiyat, A. Sali, M. Mokhtar, and F. Hashim. "Channel coding scheme for 5G mobile communication system for short length message transmission," *Wireless Personal Communications*, vol. 106, no. 2, pp. 377-400, 2019.
[19] K. Arora, J. Singh, and Y. S. Randhawa, "A survey on channel coding techniques for 5G wireless networks," *Telecommunication Systems*, vol. 73, no. 4, pp. 637-663, 2020.
[20] K. Fagervik and A. S. Larssen, "Performance and complexity comparison of low density parity check codes and turbo codes," in *Proc. Norwegian Signal Processing Symposium, (NORSIG '03)*, Bergen, Norway, Oct. 2003, pp. 2-4,

Anam Mobin was born in Aligarh, India in 1992. She received the B.Tech. degree from Aligarh Muslim University (AMU), Aligarh, India in 2014 and the M.Tech. degree from Aligarh Muslim University (AMU), Aligarh, India in 2016 both in electronics engineering. She worked as Assistant Professor in the Department of Electronics and Communication Engineering, Jamia Millia Islamia, New Delhi, India for the session 2018-1019. She is currently pursuing the Ph.D. degree with the Department of Electronics and Communication Engineering, Jamia Millia Islamia, New Delhi, India. Her research interests include wireless communication, multicarrier waveform, and channel coding techniques for 5G and future networks.

Anwar Ahmad was born in 1959. He received his B.Sc. (Engg.) degree from Aligarh Muslim University (AMU), Aligarh, India in 1983, M.E. degree from Delhi university (DU), New Delhi, India in 1998, and PhD degree from Jamia Millia Islamia (JMI), New Delhi, India in 2014 all in electronics and communication engineering. He is currently working as Professor and Head in the Department of Electronics and Communication Engineering, Jamia Millia Islamia, New Delhi, India. His research interests include 5G mobile communication, analog and digital communication, coding techniques and speech coding.